https://doi.org/10.1093/plphys/kiac482 PLANT PHYSIOLOGY 2022: 00: 1–13

Plant Physiology®

Research Article

Anatomical adjustments of the tree hydraulic pathway decrease canopy conductance under long-term elevated CO_2

Marielle Gattmann [1], Scott A. M. McAdam [2], Benjamin Birami [1], Roman Link [3], Daniel Nadal-Sala [1], Bernhard Schuldt [3], Dan Yakir [4] and Nadine K. Ruehr [1,5,*]

1 Institute of Meteorology and Climate Research – Atmospheric Environmental Research, Karlsruhe Institute of Technology, Garmisch-Partenkirchen 82467, Germany
2 Department of Botany and Plant Pathology, Purdue Center for Plant Biology, Purdue University, West Lafayette, Indiana 47907, USA
3 Ecophysiology and Vegetation Ecology, Julius-von-Sachs-Institute of Biological Sciences, University of Würzburg, Würzburg 97082, Germany
4 Department of Environmental Sciences and Energy Research, Weizmann Institute of Science, Rehovot 76100, Israel
5 Institute of Geography and Geoecology, Karlsruhe Institute of Technology, Karlsruhe 76131, Germany

*Author for correspondence: nadine.ruehr@kit.edu

M.G., D.Y., and N.K.R. designed the study. M.G., N.K.R., and B.B. conducted the experiments. R.L., D.N.S., S.A.M.M., and B.S. analyzed samples and contributed to data analyses. M.G. and N.K.R. wrote the manuscript with contributions from all co-authors.
The author responsible for distribution of materials integral to the findings presented in this article in accordance with the policy described in the Instructions for Authors (https://academic.oup.com/plphys/pages/general-instructions) is Nadine Ruehr (nadine.ruehr@kit.edu).

Abstract

The cause of reduced leaf-level transpiration under elevated CO_2 remains largely elusive. Here, we assessed stomatal, hydraulic, and morphological adjustments in a long-term experiment on Aleppo pine (*Pinus halepensis*) seedlings germinated and grown for 22–40 months under elevated (eCO_2; c. 860 ppm) or ambient (aCO_2; c. 410 ppm) CO_2. We assessed if eCO_2-triggered reductions in canopy conductance (g_c) alter the response to soil or atmospheric drought and are reversible or lasting due to anatomical adjustments by exposing eCO_2 seedlings to decreasing [CO_2]. To quantify underlying mechanisms, we analyzed leaf abscisic acid (ABA) level, stomatal and leaf morphology, xylem structure, hydraulic efficiency, and hydraulic safety. Effects of eCO_2 manifested in a strong reduction in leaf-level g_c (−55%) not caused by ABA and not reversible under low CO_2 (c. 200 ppm). Stomatal development and size were unchanged, while stomatal density increased (+18%). An increased vein-to-epidermis distance (+65%) suggested a larger leaf resistance to water flow. This was supported by anatomical adjustments of branch xylem having smaller conduits (−8%) and lower conduit lumen fraction (−11%), which resulted in a lower specific conductivity (−19%) and leaf-specific conductivity (−34%). These adaptations to CO_2 did not change stomatal sensitivity to soil or atmospheric drought, consistent with similar xylem safety thresholds. In summary, we found reductions of g_c under elevated CO_2 to be reflected in anatomical adjustments and decreases in hydraulic conductivity. As these water savings were largely annulled by increases in leaf biomass, we do not expect alleviation of drought stress in a high CO_2 atmosphere.

Introduction

Decreases in transpiration and stomatal conductance are among the most widely documented effects of elevated atmospheric [CO_2] on plants (Drake et al., 1997; Medlyn et al., 2001; Ainsworth and Rogers, 2007; Domec et al., 2017; Dusenge et al., 2019; Birami et al., 2020; Poorter et al., 2022).

Received April 11, 2022. Accepted September 24, 2022. Advance access publication October 17, 2022

Given that drought spells and extreme weather events are increasing with climate change (Seneviratne et al., 2021), quantifying that the extent to which increased CO_2 reduces plant water loss has been the objective of numerous studies over the past two decades. Results indicate that elevated CO_2 could potentially mitigate the negative effects of drought and heat in many plant species, although the extent varies depending on the type, severity, and duration of the stress (Huang and Xu, 2015; Brodribb et al., 2020). Contrastingly, it has also been observed that leaf-level responses—most prominently water savings from reduced stomatal conductance under elevated CO_2—could be counterbalanced at the plant level due to enhanced leaf growth at higher CO_2 (Tor-ngern et al., 2015; Knauer et al., 2017; Jin et al., 2018; Gattmann et al., 2021). While the body of literature on plant responses to elevated CO_2 is growing, major knowledge gaps persist (De Kauwe et al., 2021), particularly in terms of understanding the mechanisms driving the [CO_2] effect on stomatal conductance (Poorter et al., 2022).

Addressing the processes that limit stomatal conductance under elevated CO_2 is of utmost importance in a rapidly changing climate (Ainsworth and Rogers, 2007; Bonan, 2008; Jasechko et al., 2013; Klein et al., 2019). In angiosperms, there is a well-described instantaneous stomatal response to changes in atmospheric CO_2 concentration (Morison, 1985, 1987; Mott et al., 2008). Stomata in most angiosperm species will open when exposed to [CO_2] lower than ambient, and close when exposed to [CO_2] higher than ambient. The mechanism driving these responses remains relatively elusive, although recent molecular work in Arabidopsis (*Arabidopsis thaliana*) suggests that a network of core and peripheral guard cell signaling pathways drive stomatal responses to elevated CO_2 (Dubeaux et al., 2021). Nothing is known about the molecular signaling pathway for stomatal responses to [CO_2] outside of angiosperms and there appears to be a considerable evolutionary transition in stomatal responsiveness to [CO_2] across the land plant phylogeny, with angiosperm species generally having a much greater stomatal sensitivity to instantaneous changes in [CO_2] in comparison to other stomata-bearing land plants (Doi and Shimazaki, 2008; Brodribb et al., 2009; Brodribb and McAdam, 2013; Haworth et al., 2013; Franks and Britton-Harper, 2016; Kubásek et al., 2021). In angiosperms, the magnitude and speed of stomatal responses to an instantaneous change in [CO_2] are regulated by abscisic acid (ABA) levels, with enhanced responses occurring in leaves with high ABA levels (Raschke, 1975; Dubbe et al., 1978; McAdam et al., 2011; Chater et al., 2015). This augmentation of stomatal sensitivity to instantaneous changes in [CO_2] does not occur in conifers (McAdam et al., 2011), but it has never been examined whether ABA might play a role in regulating stomatal sensitivity to long-term increases in [CO_2] in conifers.

The regulation of stomatal aperture and water loss is not restricted to physiological responses but could be altered by leaf anatomical adjustments after long-term exposure to high CO_2. As widely observed, growth under elevated CO_2 may result in reduced development of stomatal complexes in the epidermis, reducing both stomatal density (SD; number of stomata per unit leaf area) and stomatal index (SI; the proportion of epidermal cells that are stomata) (Woodward and Kelly, 1995). This anatomical adjustment reduces overall stomatal conductance and increases water-use efficiency (WUE) without a change in stomatal aperture. To date, results are far from conclusive, and often have no effect, and in some cases, even an increase in SD in response to elevated CO_2 has been observed (Pritchard et al., 1999; Luomala et al., 2005; Domec et al., 2017). Hence, the magnitude of the SD response seems to be affected by the experimental setup and duration, species, and other environmental factors (Haworth et al., 2013; Xu et al., 2016). Contributing to lower SD under elevated CO_2 could be a promotion of leaf size, as observed in grasses (Xu and Zhou, 2008; Xu et al., 2014), or an increase in needle thickness or width as observed in Scots pine (*Pinus sylvestris*) (Lin et al., 2001). These changes are often related to alterations in cell division and/or cell expansion driven mainly by increased carbon availability combined with a reduction in water demand (Pritchard et al., 1999; Xu et al., 2016).

In agreement, a growing number of studies suggest that anatomical adjustments from long-term exposure to elevated CO_2 are not restricted to stomata but may affect leaf hydraulic conductance (K_{leaf}; Domec et al., 2009; Phillips et al., 2011). Increases in needle thickness and/or mesophyll tissue (Lin et al., 2001), which affect the path length the water has to travel from the vein to the stomata, have been attributed to lower K_{leaf} (Domec et al., 2016), and could be related to lower stomatal conductance as well as an enhanced WUE (Trueba et al., 2022). Moreover, a few studies have observed adjustments in xylem structure in response to elevated CO_2 (Domec et al., 2017). In conifers, structural changes were mixed and seem to vary among species, showing no responses (Maherali and DeLucia, 2000), increases in cell wall thickness (Conroy et al., 1990; Atwell et al., 2003; Kilpelainen et al., 2007; Domec et al., 2016), wood density (Telewski et al., 1999; Atwell et al., 2003), or tracheid diameter (Ceulemans et al., 2002). A recent literature review summarizes the impacts of some of these findings on tree hydraulics but no clear picture of conifers emerged. It appears that specific conductivity, that is, hydraulic conductivity normalized by xylem cross-sectional area (K_s), might slightly increase while plant hydraulic conductance and leaf water potential remain largely unchanged under elevated CO_2 (Domec et al., 2017). As the tree water transport system from roots to leaves is tightly coordinated (Meinzer and Grantz, 1990; Santiago et al., 2004; Bartlett et al., 2016), stomatal conductance could be indirectly affected by anatomical adjustments of xylem porosity, leaf thickness, or vein-to-stomata distance. The linking element here is the water status at the site of stomatal evaporation, which is influenced in part by the hydraulic conductivity of branches and leaves, and by stomatal aperture (Bartlett et al., 2016).

Furthermore, changes in whole-plant water transport capacities become likely if growth under elevated CO_2 alters xylem anatomy. These might ultimately affect the vulnerability of trees to hydraulic failure (Domec et al., 2010).

Trees growing in seasonally dry environments could be particularly affected by CO_2-induced changes that affect water demand and transport. In two previous studies, we have investigated the effect of elevated CO_2 to heat, hot drought, and lethal drought in Aleppo pine (*Pinus halepensis*) seedlings (Birami et al., 2020; Gattmann et al., 2021) grown from seeds either under ambient (aCO_2 c. 410 ppm) or highly elevated [CO_2] (eCO_2 c. 870 ppm) for 18–22 months. Seeds originated from the Yatir forest, a Aleppo pine dominated forest plantation at the northern edge of the Negev desert in Israel (Grünzweig et al., 2003). The experimental CO_2 concentrations were within the range of the RCP8.5 scenarios (794–1,142 ppm for 2,100) and hence close to CO_2 saturation for photosynthesis, providing a strong CO_2 response. Results of these two previous studies showed that elevated CO_2 enhanced whole-tree C uptake (c. + 100%), WUE, and overall tree biomass (+ 35%). Pronounced reductions in leaf-level canopy conductance (g_c) largely counterbalanced the increase in leaf area resulting in comparatively small water savings at the tree level (c. −10% at 25°C). Exposing the seedlings to heat or hot drought spells revealed little effect of elevated CO_2 on the stress response, albeit maintaining a higher WUE until respiration rates exceed photosynthesis (Birami et al., 2020). Further, elevated CO_2 did not improve the overall tree vulnerability to a lethal soil drought and the decline in leaf water potential, as well as thresholds for stomatal closure and turgor loss point, appeared unaffected (Gattmann et al., 2021). This raises the question of the underlying mechanisms that reduced g_c under elevated CO_2 and why the physiological drought response remained largely unaltered.

Here, we take advantage of this long-term elevated CO_2 experiment and assessed the coordination between anatomical and physiological adjustments of Aleppo pine seedlings from the same population grown for 22–40 months under elevated CO_2 averaging c. 860 ppm over the entire period. We studied leaf-level g_c responses to [CO_2] and increasing soil or atmospheric drought and assessed if those are coordinated by morphological changes in the hydraulic system (Figure 1). We addressed the following hypotheses: (1) stomatal closure under eCO_2 is reversible upon exposure to low CO_2 if a direct stomatal response, possibly mediated by the phytohormone ABA; (2) stomatal closure under eCO_2 is not reversible as hydraulic conductance is modified by anatomical adjustments of leaves and wood, specifically reductions in xylem tracheid diameter and SD; and (3) stomatal responses to drought and increasing vapor pressure deficit (VPD) are unaffected by elevated CO_2 and hence hydraulic vulnerability is unchanged.

Results

Long-term acclimation to elevated CO_2 affects gas exchange

Highly elevated atmospheric [CO_2] strongly reduced leaf-level gas exchange rates in Aleppo pine seedlings compared to seedlings under ambient [CO_2] (Supplemental Figure S1, a and b). These reductions were noticeable both during daytime and nighttime and $g_{c\text{-}ref}$ (g_c at a VPD of 1 kPa) was 55% lower in eCO_2 compared to aCO_2 seedlings (Table 1). But the dynamics of the diurnal cycle were not altered by the

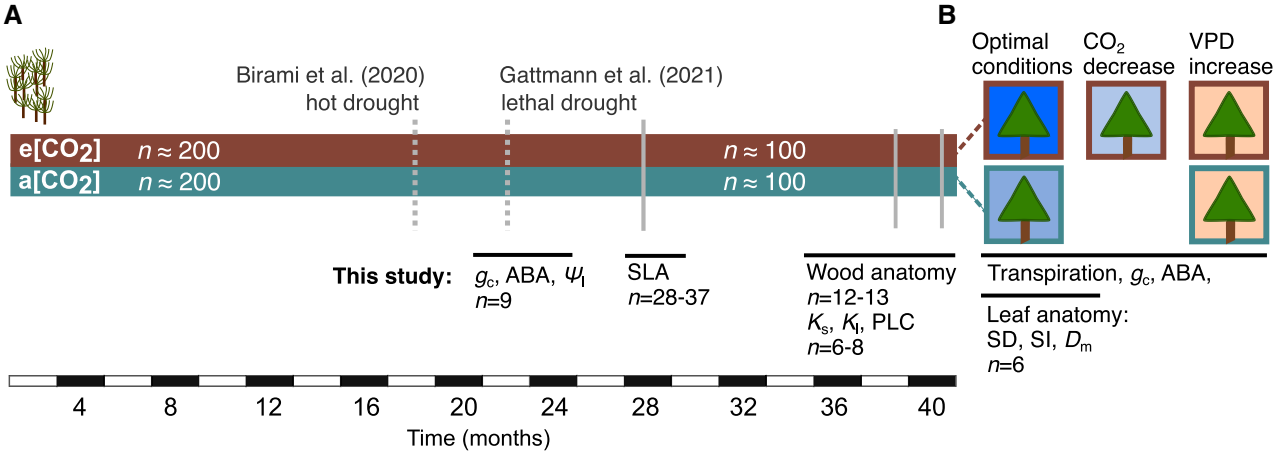

Figure 1 Timeline of cultivation of *P. halepensis* seedlings under ambient (c. 400 ppm) or (c. 860 ppm) elevated CO_2. A, The number of seedlings cultivated after germination, the conducted experiments and references, as well as measurements related to this study are shown. B, After 40 months cultivation, randomly selected seedlings (n = 6 per treatment) were placed into automated gas exchange chambers enclosing the canopy of one seedling each and transpiration and g_c were measured during optimal conditions, decreasing CO_2 (in eCO_2 seedlings only) and increasing VPD over several days alongside which leaf samples were taken to analyze for ABA content. B, This chamber system was also used to measure responses in the same population of seedlings during a dry-down experiment on 22-month-old seedlings when also leaf water potential (Ψ_l) was measured as published in Gattmann et al. (2021). Changes in leaf morphology were assessed via analyses of specific leaf area (SLA), SD, SI, and vein-to-epidermis distance (D_m). Measurements of wood anatomy included conduit diameter, lumen fraction, and potential hydraulic conductivity. Changes in hydraulic properties were assessed via measurements of specific conductivity (K_s), leaf-specific conductivity (K_l) and PLC.

Table 1 Treatment responses of leaf morphology, stomatal characteristics, reference stomatal conductance at VPD = 1 kPa ($g_{c\text{-}ref}$), and hydraulic vulnerability parameters for *P. halepensis* seedlings grown for 40 months under aCO_2 or eCO_2 atmospheric CO_2

Trait, unit	aCO_2	eCO_2
SL, µm	$51.87 \pm 5.89^{(a)}$	$55.70 \pm 8.53^{(a)}$
SD, n mm^{-2}	$28.92 \pm 3.81^{(a)}$	$35.46 \pm 4.75^{(b)}$
ED, n mm^{-2}	$133.20 \pm 15.20^{(a)}$	$166.67 \pm 20.13^{(b)}$
SI, %	$17.87 \pm 1.71^{(a)}$	$17.51 \pm 1.29^{(a)}$
D_m, µm	$150.97 \pm 9.65^{(a)}$	$252.82 \pm 6.67^{(b)}$
LW, mm	$0.85 \pm 0.05^{(a)}$	$1.19 \pm 0.05^{(b)}$
ABA, ng g^{-1} FW	$305 \pm 93^{(a)}$	$169 \pm 149^{(a)}$
LA, cm^2	$0.74 \pm 0.21^{(a)\$}$	$0.87 \pm 0.22^{(b),\#}$
SLA, cm^2 g^{-1}	$55.48 \pm 6.01^{(a)\$}$	$51.04 \pm 8.84^{(b),\#}$
$g_{c\text{-}ref}$, mol m^{-2} s^{-1}	0.2 [0.17–0.41]$^{(a)}$	0.09 [0.07–0.11]$^{(b)}$
$\Psi_{gc\text{-}close}$, –MPa	2.1 [2.20–2.00]$^{(a)}$	2.15 [2.25–2.00]$^{(a)}$
P_{12}, –MPa	3.92 [4.24–2.92]$^{(a)}$	3.33 [4.13–2.35]$^{(a)}$
P_{50}, –MPa	5.17 [5.88–4.66]$^{(a)}$	4.91 [5.96–4.19]$^{(a)}$
P_{88}, –MPa	6.11 [7.79–5.97]$^{(a)}$	6.66 [7.79–5.37]$^{(a)}$

Stomata length (SL), SD, number of ED, SI LW, and vein-to-epidermis distance (D_m), ABA, needle leaf area (LA) and SLA are mean ± SD (n = 6 per treatment if not noted otherwise). Statistical significance was tested with nonparametric Mann–Whitney U tests ($P < 0.05$). For $g_{c\text{-}ref}$, Ψ_{leaf} at stomatal closure ($\Psi_{gc\text{-}close}$) and the hydraulic vulnerability parameters (P_{12}, P_{50}, and P_{88}), the treatment median with the 95% CIs of the Bayesian model fit is given. Parameters with significant differences between treatments are highlighted in bold and indicated by different letters.
$^{\$}aCO_2$ n = 28, $^{\#}$ eCO_2 n = 37 measured in 28-month-old seedlings.

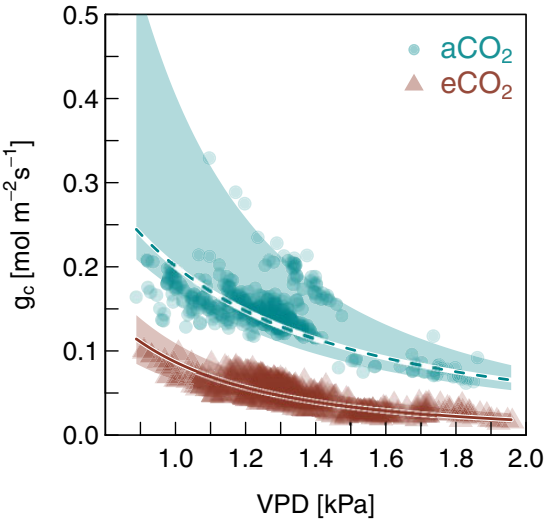

Figure 2 Treatment-specific relationships of g_c with VPD for 40-month-old *P. halepensis* seedlings grown under ambient or elevated CO_2. Shown are single measurements for six trees per treatment (aCO_2: circles; eCO_2: triangles) over the course of 3 days for PAR > 200 µmol m^{-2} s^{-1}. The trend line gives the median value of the model fit and the shaded areas represent the 95% CIs per treatment (see Supplemental Table S2 for model coefficients).

CO_2 treatment, suggesting that on a relative scale, E and g_c were affected similarly by short-term changes. This assumption was reinforced by the lack of a treatment effect in the slope of g_c responding to increasing VPD (Figure 2). In addition, reducing atmospheric [CO_2] from 900 to 400 and 200 ppm did not result in higher g_c in eCO_2 seedlings (Figure 3).

Stomata control and characteristics under elevated CO_2

Elevated CO_2-induced reductions in g_c were not driven by higher leaf ABA levels (Table 1). Moreover, the lack of a CO_2 effect on ABA levels was further confirmed as ABA levels increased with decreasing Ψ_{leaf} in both eCO_2 and aCO_2 seedlings at the same rate (Figure 4A). In addition, the stomatal aperture was tightly regulated by leaf water status, independent of the CO_2 treatment, as shown by the similar steep decline of relative g_c with Ψ_{leaf} in both treatments (Figure 4B, see also Supplemental Figure S3 for Ψ_{leaf} during dry-down). The decline in g_c with decreasing Ψ_{leaf} and the water potential at stomatal closure was comparable in both treatments (c. –2.1 MPa; Figure 4, B and C and Table 1).

To assess possible morphological adjustments in response to elevated CO_2 that could account for the reduced g_c in eCO_2 plants, we analyzed leaf and stomata morphology (Table 1). We found that growth under elevated CO_2 resulted in a significant increase in SD and epidermal pavement cell density (ED) (Table 1). As these increases in SD (+23%) and ED (+25%) were similar, there was no significant change in SI induced by elevated CO_2. We also analyzed needle width and vein-to-epidermis distance and found both to be significantly larger in leaves adapted to elevated CO_2 (Table 1). These increases in needle width corresponded to increases in individual leaf area (Table 1).

[CO_2] effect on wood anatomy and hydraulic parameters

Elevated CO_2 altered the woody anatomy of branches. As cross-sectional area had a substantial influence on all wood anatomical parameters and the samples from the different treatments differed systematically in average diameter, it was included as a covariate in the evaluation of the CO_2 effects (Figure 5). Comparing hydraulic parameters between CO_2 treatments including cross-sectional area revealed significant reductions in conduit lumen fraction (A_{lumen}, –11%; Figure 5A), average conduit diameter (D, –8%; Figure 5B), and potential conductivity (K_p, –17%; Figure 5C) of eCO_2 seedlings (generalized least square [GLS], $P < 0.05$). Conduit density (CD; Figure 5D) tended to be on average ~5% (P = 0.057) higher in eCO_2 than aCO_2, while the hydraulically weighted conduit diameter (D_h, Figure 5D) was not affected by growth CO_2.

The distinct signal of morphological changes under elevated CO_2 was also captured in specific (K_s) and leaf-specific (K_l) conductivity. Both were significantly reduced in eCO_2 plants (K_s: –19%; K_l: –34%; Mann–Whitney U test, $P < 0.05$; Figure 6, A and B). The leaf-to-sapwood area ratio (A_l:A_s, Figure 6C) tended to be larger (+24%, P = 0.090) in eCO_2 compared to aCO_2 seedlings.

Discussion

Stomatal responses to elevated CO_2

Aleppo pine seedlings grown from seeds for 40 months under highly elevated CO_2 had a 55% lower leaf-level g_c than

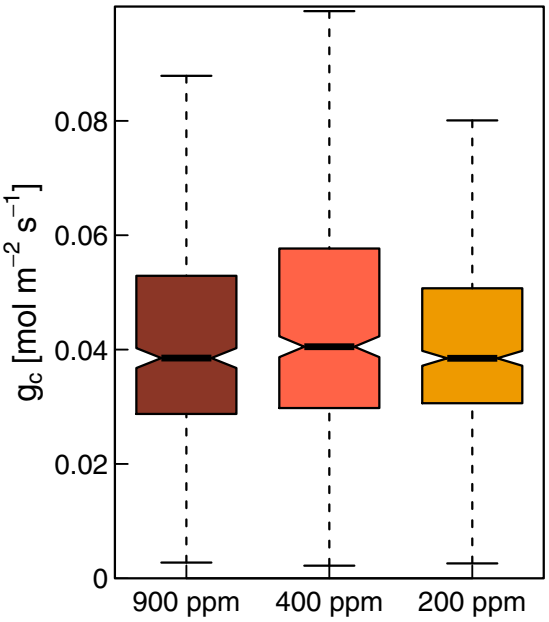

Figure 3 g_c measured at three different CO_2 concentrations of Aleppo pine seedlings grown for 40 months under elevated CO_2 (*c.* 870 ppm). In order to test whether reduced [CO_2] can trigger stomatal opening, the CO_2 seedlings (n = 6) were steadily exposed to decreasing atmospheric [CO_2] from *c.* 900, to *c.* 400, and *c.* 200 ppm and each CO_2 level was kept for 2 days. Shown are boxplots of the automated gas exchange measurements for six seedlings at PAR > 200 µmol m^{-2}s^{-1}. The box represents the interquartile range (IQR) of the data, the horizontal line at the notch is the median and the whiskers are 1.5 times the IQR. The number of measurements included were n = 481, n = 584, and n = 592 at 900, 400, and 200 ppm, respectively. Differences between CO_2 levels tested with linear mixed effect models were not significant (P > 0.05).

aCO_2 seedlings (Table 1). This reduction was 15% larger when compared to results from our previous study (Birami et al., 2020), possibly affected by the duration of CO_2 fumigation or seasonal timing of the experiment. Overall, the observed reductions in g_c exceed the average decrease of about 20% reported in many other tree species grown under elevated CO_2 (Medlyn et al., 2001; Ainsworth and Rogers, 2007; Purcell et al., 2018). These differences could be due to the high CO_2 levels of 860 ppm in our study, compared to the average of c. 570 ppm in previous studies (Ainsworth and Rogers, 2007). To further investigate the mechanism driving this considerable reduction in leaf-level g_c in Aleppo pine seedlings, we first conducted an experiment to test whether the reduced g_c was driven by a direct stomata response (Ainsworth and Rogers, 2007; Xu et al., 2016; Gamage et al., 2018; Birami et al., 2020). We found that stomata in elevated CO_2-adapted plants did not respond to [CO_2] reductions from c. 900 to 400 and 200 ppm with each level kept for 2 days (Figure 3). This suggests that stomata were not actively closed by the high CO_2 level; rather, the stomata were likely operating at an optimal level that was physiologically and anatomically determined. A similar result has been observed after 17 years of CO_2 enrichment

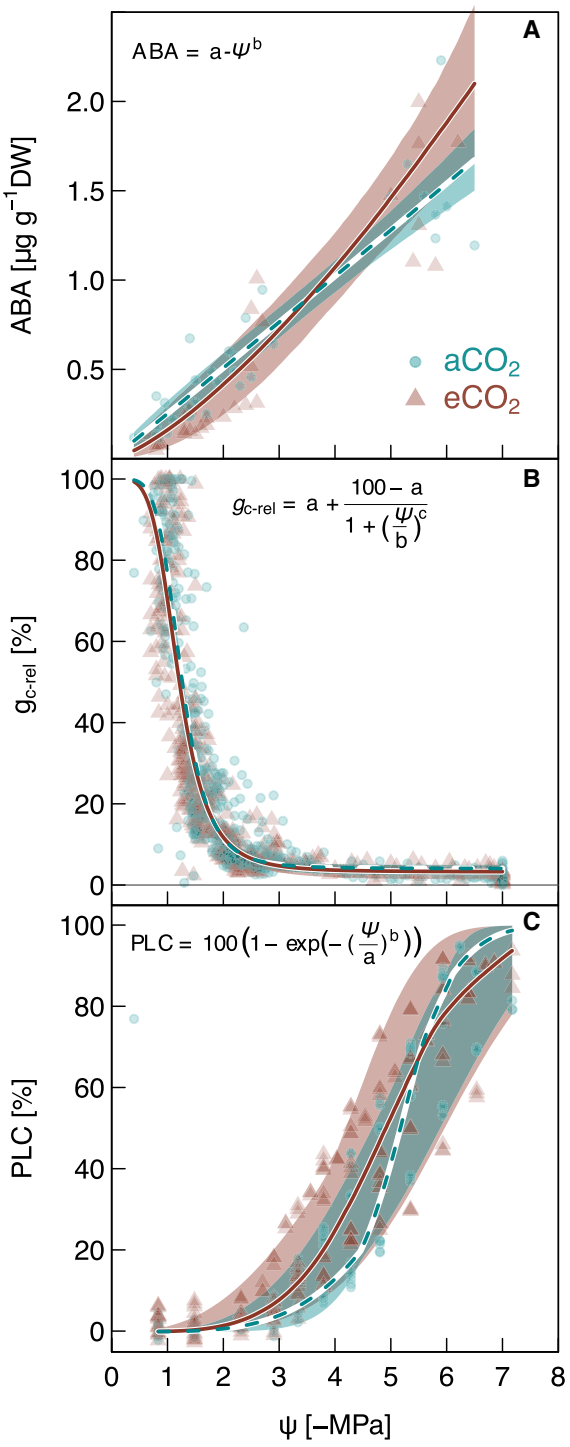

Figure 4 Hydraulic responses to increasing drought in *P. halepensis* seedlings grown under ambient or elevated CO_2. Treatment-specific relationships of (A) leaf-level ABA concentration given per dry weight (DW) needle tissue and (B) relative g_c ($g_{c\text{-}rel}$) with leaf water potential (Ψ) during a dry-down experiment are shown for the 22-month-old seedlings (n = 6 per treatment), and (C) PLC in branches versus xylem water potential (Ψ) is given for 40-month-old seedlings (aCO_2 n = 6 eCO_2 n = 8). Data points of individual measurements (aCO_2: solid points, eCO_2: solid triangles) are shown. The median of each model is indicated by solid (eCO_2) or dashed (aCO_2) lines and the shaded areas represent the 95% credible intervals per treatment (see Supplemental Table S2 for model coefficients). For values of P_{12}, P_{50}, and P_{88}, see Table 1.

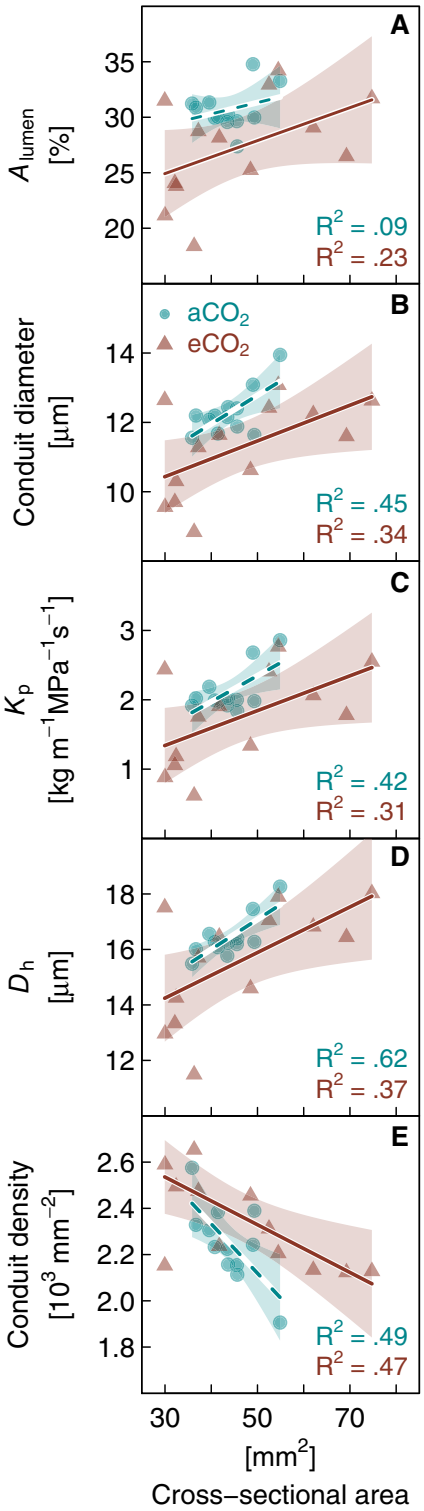

Figure 5 Wood anatomy parameters in relation to branch cross-sectional area in *P. halepensis* seedlings grown for 40 months under eCO_2 or aCO_2. A, Lumen fraction (A_{lumen}), (B) average conduit diameter, (C) potential conductivity (K_p), (D) hydraulically weighted conduit diameter (D_h), and (E) CD are given. Data are measurements of individual branch samples (n = 12–13 per treatment). Linear regressions (aCO_2: intermitted lines, eCO_2: solid lines) and the 95% confidence intervals of the fit are given (shaded areas). Note that differences between treatments were significant for A_{lumen}, conduit diameter and K_p (generalized least squares test, $P < 0.05$).

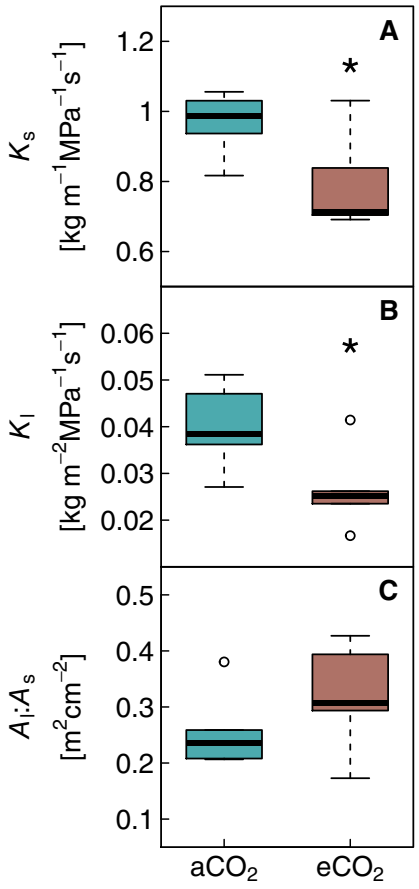

Figure 6 Responses of hydraulic conductivity and leaf-to-sapwood area in 40-month-old *P. halepensis* seedlings grown under ambient or elevated CO_2. A, Specific conductivity (K_s), (B) leaf specific conductivity (K_l), and (C) leaf-to-sapwood area ratio (A_l:A_s) are shown as boxplots per treatment (n = 6). The box represents the IQR of the data, the horizontal line inside the box is the median, the whiskers cover 1.5 times the IQR. Data points are outliers beyond the extremes of the whiskers. Significant treatment differences are indicated by asterisks (Mann–Whitney U test $P < 0.05$).

(+ 200 ppm) at the DUKE FACE site, in which [CO_2] was decreased step wise, without any indications of g_c to respond in a Loblolly pine (*Pinus taeda*) dominated stand (Tor-ngern et al., 2015). In our study, we further showed that ABA levels were not causing a direct decline of g_c under elevated CO_2, or augmenting this response as observed in angiosperms (Dubbe et al., 1978). This reinforces the assumption that the g_c reduction might be indirect (via developmental changes) rather than direct (via active stomatal aperture adjustment) and hence rejects our first hypothesis. While this contrasts observations in most angiosperm species (Giday et al., 2014; Chater et al., 2015), it is in line with previous studies which have found that conifers lack considerable instantaneous stomatal closing responses to elevated CO_2 (Brodribb et al., 2009; Brodribb and McAdam, 2013; Haworth et al., 2013).

As our 40-month-old Aleppo pine seedlings had grown their entire life under elevated CO_2, indirect responses via anatomical adjustments might be the most prominent explanation on apparent declines in g_c. We found epidermal

developmental adjustments to elevated CO_2, particularly an increased SD and ED (Table 1). This increase in SD at elevated CO_2 has rarely been documented (Ferris, 1996; Reid, 2003; Zhou et al., 2013) and is contrary to our expectation of SD reductions (Lin et al., 2001; Kouwenberg et al., 2003; Haworth et al., 2011) or no changes in SD (Apple et al., 2000; Kurepin et al., 2018). While SD and ED increased, we found SI to remain unaffected (Table 1), rejecting our hypothesis that—as in many angiosperms—a reduced initiation of stomata occurred in response to elevated CO_2 in Aleppo pine seedlings. As SD did not change independently of epidermal cell density, we suggest that the observed increase in SD was mediated by a decrease in epidermal cell expansion that led to a smaller final size of epidermal cells. Decreased epidermal cell size has been reported previously in *Phaseolus vulgaris* exposed to elevated CO_2 due to changes in both cell division and expansion (Ranasinghe and Taylor, 1996). So far, the underlying mechanisms of increased leaf cell production under elevated CO_2 are not fully resolved, but could potentially be triggered by a surplus of carbohydrates and may be linked to the increase in individual leaf size we observed in eCO_2-adapted plants.

Hydraulic conductance in leaves and branches under elevated CO_2

We found needles of eCO_2 seedlings to increase in width and cross-sectional area consequently having a longer distance for water to traverse from the vein to the substomatal cavity. Increasing the radial path length for water transport effectively limits K_{leaf} (Brodribb et al., 2010). A larger distance from the vein-to-the-epidermis has been shown to be linearly related to K_{leaf} in a range of species (Brodribb et al., 2007). This supports that K_{leaf}, although not measured directly in our study, must have been lower in eCO_2 seedlings. Moreover, an increased vein-to-epidermis distance has also been reported after long-term exposure to elevated CO_2 in Loblolly pine, which was directly related to reduced K_{leaf} and further attributed to increased resistance of outside xylem water transport (Domec et al., 2016). Similar to our study, stomata did not open when CO_2 was reduced (Tor-ngern et al., 2015). In addition, elevated CO_2 increased the needle cross-sectional area and mesophyll surface area in Scots pine (Lin et al. 2001), and recently it has been shown that a lower stomata-to-mesophyll volume ratio relates to lower stomatal conductance in conifers (Trueba et al., 2022). In Aleppo pine we found the increase in vein-to-epidermis distance (+ 65%) to be proportionally larger than the increase in SD (+ 23%), eventually contributing to a reduced g_c under elevated CO_2. Conifer leaves are not fully vascularized and as a consequence exhibit a larger difference in water potentials between veins, mesophyll, and epidermis, which may result in stomata closure even when xylem water potential is relatively high (Zwieniecki et al., 2007). Albeit leaf water potential did not differ between CO_2 treatments (Supplemental Figure S2), undetected, minor changes in localized water potential—eventually restricted to stomatal guard cells—could have resulted in turgor-driven partial stomatal closure in these conifers (McAdam and Brodribb, 2014). Additional work examining the impact of potentially altered mesophyll anatomy, transfusion tissue area, and cell size on K_{leaf} and stomatal conductance is warranted. In addition, undetected morphological changes of the stomata structure, including a greater stomatal pore depth or increases in cuticular waxes, may contribute to reduced transpiration.

We found branches of the eCO_2 seedlings to have a lower specific conductivity (K_s) and reduced leaf-specific conductivity (K_l). This was manifested in xylem morphology, reflected in a lower conduit lumen fraction and reduced average conduit diameter in branches under elevated CO_2. These anatomical changes to leaf morphology and xylem structure have likely manifested during early seedling development triggered by reduced stomatal aperture and lower water demand under high CO_2. We did not find a clear signal just a tendency of increasing leaf-to-sapwood area under eCO_2 in line with a study on cottonwood trees grown under highly elevated CO_2 (1,200 ppm) (Engel et al., 2004). This suggests that trees under elevated CO_2 allocate comparably less resources into tree water transport but more into leaf structure. At the tree level, this resulted in a larger leaf area and increased C uptake in eCO_2 plants (Supplemental Figure S3b).

These anatomical responses, as depicted, should need relatively long exposure times to elevated CO_2. For instance, in experiments on mature trees, such responses might not become apparent, as CO_2 fumigation typically spans few growing seasons and most of the woody tissue has been formed previously (e.g. Körner, 2006). This indicates that particularly in diffuse-porous and conifer species, which conduct water through multiple tree rings (Maton and Gartner, 2005), xylem hydraulic responses might only manifest after a large fraction of the woody tissue has been grown under elevated CO_2 conditions, and hence might have not been routinely observed in previous studies (Domec et al., 2017). In contrast, responses at the leaf-level should develop more quickly (e.g.Tor-ngern et al., 2015). In our study we found, albeit anatomical adjustments in leaves and xylem strongly reducing leaf-level water loss, no differences in Ψ_{leaf} and a minor response of tree-level transpiration (Supplemental Figures S2 and S3a). The reason is a pronounced increase of leaf area under eCO_2 that largely annulled leaf-level water savings (Gattmann et al., 2021). In summary, this indicates a tight coordination between anatomical adjustments and water demand in Aleppo pine seedlings grown their entire life time in a highly enriched CO_2 atmosphere.

Implications for drought and VPD responses under elevated CO_2

The rate of stomatal closure during increasing soil or atmospheric drought was not affected by elevated CO_2, albeit $g_{c\text{-}ref}$ (g_c at VPD of 1 kPa) being 55% lower in eCO_2 plants. Increasing VPD from 1 to 2 kPa resulted in a 60% reduction of g_c in both treatments. This similar g_c behaviour was reflected in ABA levels increasing as Ψ_{leaf} declined

(Figure 4), and supports previous findings of an unchanged physiological drought response in Aleppo pine grown under elevated CO_2 (Birami et al., 2020; Gattmann et al., 2021). In agreement, the hydraulic vulnerabilities reported here, indicate no differences in P_{12}, P_{50}, or P_{88} values between treatments or the water potential at stomatal closure, which supports our last hypothesis. However, it is worth mentioning that the uncertainties were relatively large and a higher number of samples would have provided larger confidence in these results. Albeit hydraulic safety was not affected, we found hydraulic efficiency to decrease under eCO_2, this was not surprising as hydraulic efficiency and safety are typically weakly linked (Gleason et al., 2016). A lower hydraulic conductivity was reflected in smaller conduits (−8%) and lower lumen fraction (−11%) of the xylem. Decreases in xylem porosity as we found under elevated CO_2 are contradictory to findings in a few conifers, which apparently tend toward larger conduit diameter and less drought-resistant xylem (Domec et al., 2017). But the results on CO_2 impacts on tree hydraulics and wood anatomy in conifers are generally mixed and sparse (Telewski et al., 1999; Olszyk et al., 2005; Domec et al., 2010) and no general picture emerges. Hence, it is worth noting that the CO_2 effects on wood anatomy as found in our study were moderate and became apparent only after accounting for the confounding effect of branch cross-sectional area, which might not routinely be considered in other studies. In summary, while some of the observed morphological adjustments could be interpreted as a protective measure, neither the hydraulic vulnerability curves nor the g_c response to increasing soil or atmospheric drought indicates an increased hydraulic safety of Aleppo pine seedlings grown under elevated CO_2.

Our study provides evidence of an unchanged metabolic and hydraulic stress response in pine seedlings grown under highly elevated CO_2. The water savings from reduced transpiration were largely compensated by an increased leaf area so that tree-level water loss was marginally lower in the eCO_2 treatment (Supplemental Figure S3) and the drought dynamics appeared unchanged (Gattmann et al., 2021). Based on these results, we suggest that drought responses of mature trees in the field should depend on leaf area stimulations from elevated CO_2 (De Kauwe et al., 2021), which in turn affects tree and forest water demand. For instance, if an increase in leaf area balances CO_2-induced reductions in water loss, tree or ecosystem-level drought progression should be unchanged. In contrast, if the leaf area does not respond to elevated CO_2, the CO_2-induced leaf-level water savings as observed here have the potential to buffer forest drought progression as soil water resources should deplete more slowly.

Materials and methods

Plant material

Aleppo pine seedlings were cultivated from seed either under ambient (on average 410 ± 23 ppm) or elevated (on average 860 ± 15 ppm) [CO_2] for 40 months in a greenhouse facility in Garmisch-Partenkirchen, Germany (732 m a.s.l., 47°28′49.2″N, 35°3′7.2″E). Other environmental drivers such as air temperature (daytime c. 22°C ± 2.5°C, nighttime 15°C ± 2°C), relative humidity (75% ± 15%), photosynthetically active radiation (PAR; 480 ± 180 µmol m^{-2} s^{-1}), and water availability (watered daily to full saturation) were maintained at similar levels in both CO_2 treatments, and the mean difference between daily mean air temperature was typically < 1°C. Winter periods (months December to February) were mimicked in the greenhouse by reducing daily air temperature to 12°C on average. The placement of the seedlings was repeatedly changed between and within the greenhouse compartments. During the initial 24 months of cultivation, the seedlings were placed in pots and repotted twice (last into 4.5-L pots). The potting substrate, a mixture of quartz sand, vermiculite, and expanded clay, was repeatedly enriched with slow-release fertilizer (Osmocote Exact Standard 5-6M 15-9-12 + 2MgO + TE; ICL Specialty Fertilizers) and supplemented by liquid fertilizer during the growing period. Initially, about 200 seedlings were grown under aCO_2 or eCO_2 to ensure a large enough population from which to randomly select seedlings for stress experiments involving destructive sampling. More details on seedling cultivation and experiments can be found in the two previously published studies, which used seedlings from the same population (Birami et al., 2020; Gattmann et al., 2021).

Experimental setup and growth conditions

We assessed stomatal responses in eCO_2- and aCO_2-grown seedlings to drought, VPD, and decreasing [CO_2] using custom-made gas exchange chambers (Birami et al., 2020; Gattmann et al., 2021; Rehschuh et al., 2022) consisting of a tightly sealed shoot compartment separated from the root compartment. In brief, each of the shoot compartments was made of a light-transmitting cylinder and was individually temperature controlled and equipped with temperature sensors (5SC-TTTI-36-2 M, Newport Electronics GmbH, Deckenpfronn, Germany). The drought experiment was conducted in early 2018 when the seedlings (n = 9 per treatment) were ∼22-month old (see Figure 6) as described in detail by Gattmann et al. (2021). The VPD and decreasing CO_2 experiments were conducted later on 40-month-old seedlings in September 2019. Prior to experiments, we randomly selected six seedlings per treatment (each ∼50 cm tall). We conducted the experiments in a sequence starting with the eCO_2 seedlings followed by aCO_2 seedlings. Each seedling was placed into one of the six individual gas exchange chambers with the shoot compartment tightly sealed from the belowground part of the plant. Ambient sunlight was supplemented by plant growth lamps (T-agro 400 W; Philips, Hamburg, Germany), ensuring a relatively constant average PAR (PQS 1, Kipp & Zonen, Delft, the Netherlands) of 450 ± 50 µmol m^{-2} s^{-1} over each 16-h day measurement period (Supplemental Figure S1, c and d). All seedlings were automatically drip irrigated daily to field capacity.

Gas exchange measurements

To test for reversibility in the restriction on g_c in eCO_2 plants, $[CO_2]$ was reduced as follows. After the shoot of each seedling was placed into an individual gas exchange chamber, elevated CO_2 was maintained for 3 days at 854 ± 29 ppm, then $[CO_2]$ was reduced close to ambient concentrations (382 ± 19 ppm) and then to 199 ± 9 ppm, maintaining each $[CO_2]$ change for 2 days. All other chamber conditions were kept constant with the day-time VPD at 1.34 ± 0.22 kPa and day-time air temperature at $24.2°C \pm 0.49°C$ (min/max: 21.9°C/25.9°C). Nighttime temperature was maintained at $19.70°C \pm 0.58°C$. Temperature variations between chambers were small ($<2°C$).

We evaluated the responses of g_c in eCO_2 seedlings to changes in VPD during 3 days under elevated CO_2 (841 ± 23 ppm). VPD was allowed to vary diurnally from 0.9 kPa to 2.1 kPa while air temperature was maintained almost constant (min/max: 23.0°C/24.7°C). Following the removal of the eCO_2 seedlings from the chambers, the aCO_2 seedlings were installed, and g_c responses to VPD were assessed over three consecutive days at ambient CO_2 (432 ± 17 ppm) with VPD ranging from 0.8 to 2.0 kPa, while air temperature was maintained relatively constant (min/max: 22.0°C/25.8°C).

Canopy H_2O gas exchange ($n = 6$ per treatment) was derived by directly measuring absolute $[CO_2]$ and $[H_2O]$ of the 10 L min^{-1} supply air stream (LI-840, Li-cor, Lincoln, NE) and the concentration differences between supply and sample air stream (Li-7000, Li-cor, Lincoln, NE). Data were recorded every 10 s while the system automatically switched between chambers every 120 s so that each chamber was measured at least half-hourly. The last 40 s of each measurement was used to calculate net photosynthesis, transpiration, and g_c. Two empty chambers were additionally integrated into the measurement cycle to continuously monitor the system and correct the data for any fluctuations in $[H_2O]$ that were not due to plant activity and these were typically small (0.03 ± 0.20 ppt H_2O).

To quantify g_c to water vapor we derived leaf-level transpiration rate (E) in [mol $m^{-2}s^{-1}$] as follows:

$$E = \frac{F_m(W_{supply} - W_{sample})}{A_{leaf}(1 - W_{sample})}, \quad (1)$$

where W_{supply} [mol mol^{-1}] is $[H_2O]$ in supply air stream, W_{sample} [mol mol^{-1}] is $[H_2O]$ in sample air stream, F_m [mol s^{-1}] is molar flow and A_{leaf} [m^2] is the two-dimensional leaf surface area of the shoot.

Canopy stomatal conductance (g_c; [mol H_2O m^{-2} s^{-1}]) was then calculated from leaf-level transpiration and water vapor concentration using the following equation:

$$g_c = \frac{E\left(1 - \frac{W_{leaf} + W_{sample}}{2}\right)}{W_{leaf} - W_{sample}}, \quad (2)$$

where W_{leaf} is leaf saturated vapor pressure, derived from saturation vapor pressure (kPa) at a given air temperature (°C) and atmospheric pressure. Boundary layer conductance was neglected due to high mixing conditions generated from fans and high flow rates inside the chambers (Birami et al., 2020).

To determine leaf area at the end of the gas exchange measurements, all leaves were harvested, dried at 60°C for 48 h and weighed. Leaf biomass was then multiplied by specific leaf area, previously determined from a subsample of needles.

Tissue sampling for anatomy and hormone analysis

Leaves for ABA quantification and epidermal anatomy were sampled randomly from each of the seedlings in the gas exchange chambers ($n = 6$ per treatment). The sampling was conducted between 12:00 and 14:00, and leaf samples (4–6 fascicles each) were weighed and placed either in 80% methanol in water (v/v) (for ABA analysis) or ethanol (for anatomical analysis). In addition, leaves were sampled for ABA analysis during the course of a previously conducted drought experiment (Gattmann et al., 2021). These leaf samples ($n = 18$ per treatment), initially snap-frozen in liquid nitrogen and stored at −80°C, were then transferred to 80% methanol in water (v/v) while still frozen for ABA analysis. During this previous drought experiment, midday leaf water potential (Ψ_{leaf}) was intensively measured during the dry-down.

Quantification of foliage ABA levels

Foliage ABA levels were quantified by physicochemical methods with an added internal standard. Samples were homogenized and 15 ng of [$^2H_6$]ABA was added to each sample as an internal standard. Endogenous ABA was extracted from homogenized tissue overnight at 4°C. An aliquot was taken and dried under vacuum until completeness. Samples were resuspended in 200 µL of 2% acetic acid in water (v/v), and hormone levels were quantified using liquid chromatography–mass spectrometry (Agilent 6400 series triple quadrupole LC/MS, USA) (McAdam and Brodribb, 2015).

Epidermal and leaf cross-sectional anatomy

To assess changes in stomatal development, the cuticle morphology of the sampled leaves was studied. Briefly, leaf cuticles of the central 1 cm of a needle were prepared by making a longitudinal section through one corner of the leaf and then macerating the sample in aqueous chromium trioxide. Cuticles were mounted in glycerine jelly and imaged under 10× magnification for epidermal and stomatal cell density determination with care taken to avoid leaf margins, and 40× magnification for stomatal size measurements (AxioImagerA2, Zeiss, Germany). Stomatal size was determined as the length of the stomatal complex. The mean stomatal and epidermal cell density of the whole leaf was quantified as the number of cells per square millimeter from five images per cuticle. SI, that is, the ratio of SD to ED was calculated for each image as follows:

$$SI\ (\%) = 100 \cdot \frac{SD}{SD + ED} \quad (3)$$

Leaf width (LW) was measured on the same leaves using high-precision calipers (±0.01 mm). These leaves were also cross-sectioned to measure the shortest distance between the vein-to-the-stomata-bearing epidermis using a freezing stage microtome, stained with dilute aqueous toluene blue, and mounted in glycerine jelly for imaging as above.

Hydraulic conductivity, xylem vulnerability curves, and wood anatomy

Branches for hydraulic analysis were taken in August and October 2019 from seedlings of the same population but were not part of the gas exchange measurements. These branch samples were immediately wrapped in foil and kept moist until analysis was conducted 2–3 days later. Maximal hydraulic conductivity (K_h, kg m MPa^{-1} s^{-1}) was measured in six stem segments (mean diameter ± SE: 7.33 ± 0.18 mm) per treatment after vacuum infiltration for 24 h at 30 mbar in the degassed solution of 10-mM KCl and 1-mM $CaCl_2$ in demineralized water filtered to a particle size of 0.2 µm. The segments were recut underwater to a length of 73.91 ± 1.31 mm (mean ± SE) with a sharp razor blade, connected to a Xyl'em Plus device (Bronkhorst France, Montigny les Cormeilles, France), and hydraulic conductivity was measured in the measurement solution described above. K_h was recorded at a pressure head of 4 kPa with the XylWin version 3.0 software (Bronkhorst France, Montigny les Cormeilles, France). Subsequently, we estimated specific conductivity (K_s, kg m^{-1} MPa^{-1} s^{-1}) from K_h divided by the cross-sectional area, and leaf-specific conductivity (K_l, kg m^{-1} MPa^{-1} s^{-1}) from K_h divided by the leaf area supported by the corresponding branch. The needle area of each branch was estimated from needle dry weight and treatment-averaged specific leaf area.

Xylem vulnerability curves were constructed for stem segments (aCO_2: $n = 5$; eCO_2: $n = 6$) with the flow-centrifuge technique (Cavitron; Cochard et al., 2005). Stem segments (mean basipetal diameter ± SE: 7.25 ± 0.33 mm) were shorted to 27.5 cm under water and inserted in a custom-made rotor attached to an ultra-centrifuge (Sorvall RC-5C, Thermo Fisher Scientific, Waltham, MA, USA). Conductivity measurements started at −0.84 MPa and were repeated under increasingly negative water potentials until PLC (%) reached at least 90%. We fitted Weibull functions to describe the relationship between PLC and xylem pressure (Nadal-Sala et al., 2021).

From all segments used for xylem hydraulic measurements (aCO_2: $n = 12$; eCO_2: $n = 13$), semi-thin transverse sections were cut with a sliding microtome (G.S.L.1, Schenkung Dapples, Zurich, Switzerland), stained with safranin, and the complete cross-section digitalized at 100 × magnification using a light microscope (Observer Z1, Carl Zeiss MicroImaging GmbH, Jena, Germany) equipped with an automated stage. Per segment, 51,242 ± 5,978 conduits (mean ± SE) were analyzed on average. Image processing was performed with the open-source software Gimp (https://www.gimp.org) and ImageJ (Schneider et al., 2012) using the particle analysis function. Measured parameters included the conduit lumen-to-sapwood area ratio (A_{lumen}, %), CD (n mm^{-2}), and conduit diameter (D, µm) from major (1) and minor (2) conduit radii according to $D = ((32 \times (a \times b)^3)/(a^2 + b^2))^{1/4}$, the hydraulically weighted diameter (D_h, µm) as $Dh = \Sigma D^5/\Sigma D^4$ (Sperry and Saliendra, 1994) and potential hydraulic conductivity (K_p, kg m^{-1} MPa^{-1} s^{-1}) were calculated with the Hagen–Poiseuille equation as $KP = (\pi \times \rho \times \Sigma D^4)/(128\,\eta \times A_{xylem})$, where η is the viscosity ($1.002\ 10^{-9}$ MPa s) and ρ the density of water (998.2 kg m^{-3}), both at 20°C, and A_{xylem} (m^2) the sapwood area.

Statistical analyses

Statistical analyses were conducted using R version 4.04 (R Core Team 2021). Differences in hydraulic parameters (K_s, K_l, and A_l:A_s), needle, and stomatal morphology were tested using nonparametric Mann–Whitney U tests. Wood anatomy parameters were assessed via GLS models (package nlme, Pinheiro et al., 2021). As wood anatomical traits closely covaried with branch thickness, their centered, natural log-transformed cross-sectional area was included as a covariate. Further, the residual variance was allowed to differ between treatments to account for inhomogeneous variances. We tested differences in the response of g_c to step-wise changes in CO_2 concentrations (900, 400, or 200 ppm) using linear mixed effect models (package lme4; Bates et al., 2015) with tree as a random factor. The most parsimonious model was selected based on the Akaike information criterion.

We applied Bayesian statistics to address treatment differences of nonlinear relationships (BayesianTools package, Hartig et al., 2019). This included hydraulic vulnerability curves, responses of g_c with VPD, and Ψ_{leaf} and of ABA with Ψ_{leaf} (for model details see Supplemental Methods S1). We started with broad uniform but biologically meaningful priors (Supplemental Table S1) assuming a Gaussian likelihood and used a Differential-Evolution Markov Monte Carlo Chain with memory and a snooker update following the approach by Braak and Vrugt (2008). The posterior was obtained for each calibration (30,000 iterations) with a burn-in of 10,000 samples. We assessed between-chain convergence via the Gelman–Rubin diagnostic at $\leqslant 1.1$ (Gelman and Rubin, 1992). In the case where we derived individual posteriors per tree seedling, these were later merged into a combined posterior distribution per treatment. Posterior predictive uncertainty was addressed by sampling 5,000 times the combined posterior. For each parameter, we report the median and 95% credible intervals. We considered differences between treatments to be meaningful if the CI between treatments did not overlap (see Supplemental Table S2 for model coefficients).

Supplemental data

The following materials are available in the online version of this article.

Supplemental Methods S1. Nonlinear model fitting.

Supplemental Table S1. Prior distributions of the Bayesian model calibrations.

Supplemental Table S2. Parameter estimates of the Bayesian models.

Supplemental Figure S1. Leaf-level gas exchange.

Supplemental Figure S2. Midday leaf water potential during soil drought.

Supplemental Figure S3. Tree-level transpiration and photosynthesis.

Acknowledgments

We are grateful to Nils Risse, Stefanie Dumberger, Johanna Schurr, and Andreas Gast for experimental support. We acknowledge the use of the Metabolite Profiling facility of the Bindley Bioscience Center, a core facility of the National Institute of Health-funded Indiana Clinical and Translational Sciences Institute, for assisting in the quantification of ABA levels.

Funding

This study was supported by the German Research Foundation through its Emmy Noether Program (RU 1657/2-1), the German Research Foundation through its German-Israeli project cooperation program (SCHM 2736/2-1 and YA 274/1-1), the Alexander von Humboldt Foundation through a Fellowship to S.M., and the USDA National Institute of Food and Agriculture (Hatch project 1014908).

Conflict of interest statement. None declared.

References

Ainsworth EA, Rogers A (2007) The response of photosynthesis and stomatal conductance to rising [CO2]: mechanisms and environmental interactions: photosynthesis and stomatal conductance responses to rising [CO2]. Plant Cell Environ **30**: 258–270

Apple O, Ormrod L, Southworth T (2000) Morphology and stomatal function of douglas-fir needles exposed to climate change: elevated CO2 and temperature. Int J Plant Sci **161**: 127–132

Atwell BJ, Henery ML, Whitehead D (2003) Sapwood development in *Pinus radiata* trees grown for three years at ambient and elevated carbon dioxide partial pressures. Tree Physiol **23**: 13–21

Bartlett MK, Klein T, Jansen S, Choat B, Sack L (2016) The correlations and sequence of plant stomatal, hydraulic, and wilting responses to drought. Proc Natl Acad Sci **113**: 13098–13103

Bates D, Mächler M, Bolker B, Walker S (2015) Fitting linear mixed-effects models using lme4. J Statist Softw **67**: 1–48

Birami B, Nägele T, Gattmann M, Preisler Y, Gast A, Arneth A, Ruehr NK (2020) Hot drought reduces the effects of elevated CO2 on tree water-use efficiency and carbon metabolism. New Phytologist **226**: 1607–1621

Bonan GB (2008) Forests and climate change: forcings, feedbacks, and the climate benefits of forests. Science **320**: 1444–1449

Braak CJFT, Vrugt JA (2008) Differential Evolution Markov Chain with snooker updater and fewer chains. Statist Comput **18**: 435–446

Brodribb TJ, Feild TS, Jordan GJ (2007) Leaf maximum photosynthetic rate and venation are linked by hydraulics. Plant Physiol **144**: 1890–1898

Brodribb TJ, Feild TS, Sack L (2010) Viewing leaf structure and evolution from a hydraulic perspective. Funct Plant Biol **37**: 488–498

Brodribb TJ, McAdam SAM (2013) Unique responsiveness of angiosperm stomata to elevated CO2 explained by calcium signalling. PLoS One **8**: e82057

Brodribb TJ, McAdam SAM, Jordan GJ, Feild TS (2009) Evolution of stomatal responsiveness to CO2 and optimization of water-use efficiency among land plants. New Phytologist **183**: 839–847

Brodribb TJ, Powers J, Cochard H, Choat B (2020) Hanging by a thread? Forests and drought. Science **368**: 261–266

Ceulemans R, Jach ME, van de Velde R, Lin JX, Stevens M (2002) Elevated atmospheric CO2 alters wood production, wood quality and wood strength of Scots pine (*Pinus sylvestris* L) after three years of enrichment. Glob Change Biol **8**: 153–162

Chater C, Peng K, Movahedi M, Dunn JA, Walker HJ, Liang YK, McLachlan DH, Casson S, Isner JC, Wilson I, et al. (2015) Elevated CO2 - Induced responses in stomata require ABA and ABA signaling. Curr Biol **25**: 2709–2716

Cochard H, Damour G, Bodet C, Tharwat I, Poirier M, Améglio T (2005) Evaluation of a new centrifuge technique for rapid generation of xylem vulnerability curves. Physiol Plant **124**: 410–418

Conroy JP, Milham PJ, Mazur M, Barlow EWR (1990) Growth, dry weight partitioning and wood properties of *Pinus radiata* D. Don after 2 years of CO2 enrichment. Plant Cell Environ **13**: 329–337

De Kauwe MG, Medlyn BE, Tissue DT (2021) To what extent can rising [CO2] ameliorate plant drought stress? New Phytologist **231**: 2118–2124

Doi M, Shimazaki K-i (2008) The stomata of the fern Adiantum capillus-veneris do not respond to CO2 in the dark and open by photosynthesis in guard cells. Plant Physiol **147**: 922–930

Domec JC, Palmroth S, Oren R (2016) Effects of *Pinus taeda* leaf anatomy on vascular and extravascular leaf hydraulic conductance as influenced by N-fertilization and elevated CO2. J Plant Hydraulics **3**: e007

Domec JC, Palmroth S, Ward E, Maier CA, Thérézien M, Oren R (2009) Acclimation of leaf hydraulic conductance and stomatal conductance of *Pinus taeda* (Loblolly pine) to long-term growth in elevated CO2 (free-air CO2 enrichment) and N-fertilization. Plant Cell Environ **32**: 1500–1512

Domec JC, Schafer K, Oren R, Kim HS, McCarthy HR (2010) Variable conductivity and embolism in roots and branches of four contrasting tree species and their impacts on whole-plant hydraulic performance under future atmospheric CO2 concentration. Tree Physiol **30**: 1001–1015

Domec JC, Smith DD, McCulloh KA (2017) A synthesis of the effects of atmospheric carbon dioxide enrichment on plant hydraulics: implications for whole-plant water use efficiency and resistance to drought: CO2 effects on plant hydraulics. Plant Cell Environ **40**: 921–937

Drake BG, Gonzàlez-Meler MA, Long SP (1997) More efficient plants: a consequence of rising atmospheric CO2? Ann Rev Plant Physiol Plant Mol Biol **48**: 609–639

Dubbe DR, Farquhar GD, Raschke K (1978) Effect of abscisic acid on the gain of the feedback loop involving carbon dioxide and stomata. Plant Physiol **62**: 413–417

Dubeaux G, Hsu PK, Ceciliato PH, Swink KJ, Rappel WJ, Schroeder JI (2021) Deep dive into CO2-dependent molecular mechanisms driving stomatal responses in plants. Plant Physiol **187**: 2032–2042

Dusenge ME, Duarte AG, Way DA (2019) Plant carbon metabolism and climate change: elevated CO2 and temperature impacts on photosynthesis, photorespiration and respiration. New Phytologist **221**: 32–49

Engel VC, Griffin KL, Murthy R, Patterson L, Klimas C, Potosnak M (2004) Growth CO2 concentration modifies the transpiration response of Populus deltoides to drought and vapor pressure deficit. Tree Physiol **24**: 1137–1145

Ferris R (1996) Elevated CO2 and temperature have different effects on leaf anatomy of perennial ryegrass in spring and summer. Ann Bot **78**: 489–497

Franks PJ, Britton-Harper ZJ (2016) No evidence of general CO2 insensitivity in ferns: one stomatal control mechanism for all land plants? New Phytologist **211**: 819–827

Gamage D, Thompson M, Sutherland M, Hirotsu N, Makino A, Seneweera S (2018) New insights into the cellular mechanisms of plant growth at elevated atmospheric carbon dioxide concentrations: elevated CO2 effect on plant growth and development. Plant Cell Environ **41**: 1233–1246

Gattmann M, Birami B, Nadal Sala D, Ruehr NK (2021) Dying by drying: timing of physiological stress thresholds related to tree death is not significantly altered by highly elevated CO2. Plant Cell Environ **44**: 356–370

Gelman A, Rubin DB (1992) Inference from iterative simulation using multiple sequences. Statist Sci **7**: 457–472

Giday H, Fanourakis D, Kjaer KH, Fomsgaard IS, Ottosen CO (2014) Threshold response of stomatal closing ability to leaf abscisic acid concentration during growth. J Exp Bot **65**: 4361–4370

Gleason SM, Westoby M, Jansen S, Choat B, Hacke UG, Pratt RB, Bhaskar R, Brodribb TJ, Bucci SJ, Cao KF (2016) Weak tradeoff between xylem safety and xylem-specific hydraulic efficiency across the world's woody plant species. New Phytologist **209**: 123–136

Grünzweig JM, Lin T, Rotenberg E, Schwartz A, Yakir D (2003) Carbon sequestration in arid-land forest. Glob Change Biol **9**: 791–799

Hartig F, Minunno F, Paul S (2019) BayesianTools: General-Purpose MCMC and SMC Samplers and Tools for Bayesian Statistics. R package version 0.1.7

Haworth M, Elliott-Kingston C, McElwain JC (2011) The stomatal CO2 proxy does not saturate at high atmospheric CO2 concentrations: evidence from stomatal index responses of Araucariaceae conifers. Oecologia **167**: 11–19

Haworth M, Elliott-Kingston C, McElwain JC (2013) Co-ordination of physiological and morphological responses of stomata to elevated CO2 in vascular plants. Oecologia **171**: 71–82

Huang B, Xu Y (2015) Cellular and molecular mechanisms for elevated CO2 -regulation of plant growth and stress adaptation. Crop Sci **55**: 1405–1424

Jasechko S, Sharp ZD, Gibson JJ, Birks SJ, Yi Y, Fawcett PJ (2013) Terrestrial water fluxes dominated by transpiration. Nature **496**: 347–350

Jin Z, Ainsworth EA, Leakey ADB, Lobell DB (2018) Increasing drought and diminishing benefits of elevated carbon dioxide for soybean yields across the US Midwest. Glob Change Biol **24**: e522–e533

Kilpelainen A, Gerendiain AZ, Luostarinen K, Peltola H, Kellomaki S (2007) Elevated temperature and CO2 concentration effects on xylem anatomy of Scots pine. Tree Physiol **27**: 1329–1338

Klein T, Ramon U, McCulloh K (2019) Stomatal sensitivity to CO2 diverges between angiosperm and gymnosperm tree species. Funct Ecol **33**: 1411–1424

Knauer J, Zaehle S, Reichstein M, Medlyn BE, Forkel M, Hagemann S, Werner C (2017) The response of ecosystem water–use efficiency to rising atmospheric CO2 concentrations: sensitivity and large-scale biogeochemical implications. New Phytologist **213**: 1654–1666

Körner C (2006) Plant CO2 responses: an issue of definition, time and resource supply. New Phytologist **172**: 393–411

Kouwenberg LLR, McElwain JC, Kurschner WM, Wagner F, Beerling DJ, Mayle FE, Visscher H (2003) Stomatal frequency adjustment of four conifer species to historical changes in atmospheric CO2. Am J Bot **90**: 610–619

Kubásek J, Hájek T, Duckett J, Pressel S, Šantrůček J (2021) Moss stomata do not respond to light and CO2 concentration but facilitate carbon uptake by sporophytes: a gas exchange, stomatal aperture, and 13C-labelling study. New Phytologist **230**: 1815–1828

Kurepin LV, Stangl ZR, Ivanov AG, Bui V, Mema M, Hüner NPA, Öquist G, Way D, Hurry V (2018) Contrasting acclimation abilities of two dominant boreal conifers to elevated CO2 and temperature: CO2 and warming effects on spruce and pine. Plant Cell Environ **41**: 1331–1345

Lin J, Jach ME, Ceulemans R (2001) Stomatal density and needle anatomy of Scots pine (*Pinus sylvestris*) are affected by elevated CO2. New Phytologist **150**: 665–674

Luomala EM, Laitinen K, Sutinen S, Kellomaki S, Vapaavuori E (2005) Stomatal density, anatomy and nutrient concentrations of Scots pine needles are affected by elevated CO2 and temperature. Plant Cell Environ **28**: 733–749

Maherali H, DeLucia EH (2000) Interactive effects of elevated CO2 and temperature on water transport in ponderosa pine. Am J Bot **87**: 243–249

Maton C, Gartner BL (2005) Do gymnosperm needles pull water through the xylem produced in the same year as the needle? Am J Bot **92**: 123–131

McAdam SA, Brodribb TJ (2014) Separating active and passive influences on stomatal control of transpiration. Plant Physiol **164**: 1578–1586

McAdam SA, Brodribb TJ, Ross JJ, Jordan GJ (2011) Augmentation of abscisic acid (ABA) levels by drought does not induce short-term stomatal sensitivity to CO2 in two divergent conifer species. J Exp Bot **62**: 195–203

McAdam SAM, Brodribb TJ (2015) The evolution of mechanisms driving the stomatal response to vapor pressure deficit. Plant Physiol **167**: 833–843

Medlyn BE, Barton CVM, Broadmeadow MSJ, Ceulemans R, Angelis PD, Forstreuter M, Freeman M, Jackson SB, Kellomäki S, Laitat E, et al. (2001) Stomatal conductance of forest species after long-term exposure to elevated CO2 concentration: a synthesis. New Phytologist **149**: 247–264

Meinzer FC, Grantz DA (1990) Stomatal and hydraulic conductance in growing sugarcane: stomatal adjustment to water transport capacity. Plant Cell Environ **13**: 383–388

Morison JI (1985) Sensitivity of stomata and water use efficiency to high CO2. Plant Cell Environ **8**: 467–474

Morison JI (1987) Intercellular CO2 concentration and stomatal response to CO2. Stomatal Function. Stanford University Press, Stanford, CA, pp. 229–251

Mott KA, Sibbernsen Ed Fau - Shope JC, Shope JC (2008) The role of the mesophyll in stomatal responses to light and CO2. Plant Cell Environ **31**: 1299–1306

Nadal-Sala D, Grote R, Birami B, Knüver T, Rehschuh R, Schwarz S, Ruehr NK (2021) Leaf Shedding and non-stomatal limitations of photosynthesis itigate hydraulic conductance losses in scots pine saplings during severe drought stress. Front Plant Sci **12**: 715127

Olszyk D, Apple M, Gartner B, Spicer R, Wise C, Buckner E, Benson-Scott A, Tingey D (2005) Xeromorphy increases in shoots of Pseudotsuga menziesii (Mirb.) Franco seedlings with exposure to elevated temperature but not elevated CO2. Trees **19**: 552–563

Phillips NG, Attard RD, Ghannoum O, Lewis JD, Logan BA, Tissue DT (2011) Impact of variable [CO2] and temperature on water transport structure–function relationships in Eucalyptus. Tree Physiol **31**: 945–952

Pinheiro J, Bates D, DebRoy S, Sarkar D, R Core Team. (2021) nlme: Linear and Nonlinear Mixed Effects Models. R package version 3.1-152. https://CRAN.R-project.org/package=nlme (February 4, 2021)

Poorter H, Knopf O, Wright IJ, Temme AA, Hogewoning SW, Graf A, Cernusak LA, Pons TL (2022) A meta-analysis of responses of C3 plants to atmospheric CO2: dose–response curves for 85 traits ranging from the molecular to the whole-plant level. New Phytologist **233**: 1560–1596

Pritchard SG, Rogers HH, Prior SA, Peterson CM (1999) Elevated CO2 and plant structure: a review. Glob Change Biol **5**: 807–837

Purcell C, Batke S, Yiotis C, Caballero R, Soh W, Murray M, McElwain JC (2018) Increasing stomatal conductance in response to rising atmospheric CO2. Ann Bot **121**: 1137–1149

Ranasinghe S, Taylor G (1996) Mechanism for increased leaf growth in elevated CO2. J Exp Bot **47**: 349–358

Raschke K (1975) Simultaneous requirement of carbon dioxide and abscisic acid for stomatal closing in Xanthium strumarium L. Planta **125**: 243–259

Rehschuh R, Rehschuh S, Gast A, Jakab AL, Lehmann MM, Saurer M, Gessler A, Ruehr NK (2022) Tree allocation dynamics beyond heat and hot drought stress reveal changes in carbon storage, belowground translocation and growth. New Phytologist **233**: 687–704

Reid CD (2003) On the relationship between stomatal characters and atmospheric CO2. Geophys Res Lett **30**: 1983

Santiago LS, Goldstein G, Meinzer FC, Fisher JB, Machado K, Woodruff D, Jones T (2004) Leaf photosynthetic traits scale with hydraulic conductivity and wood density in Panamanian forest canopy trees. Oecologia **140**: 543–550

Schneider CA, Rasband WS, Eliceiri KW (2012) NIH Image to ImageJ: 25 years of image analysis. Nat Methods **9**: 671–675

Seneviratne SI, Zhang X, Adnan M, Badi W, Dereczynski C, Di Luca A, Ghosh S, Iskandar I, Kossin J, Lewis S et al. (2021) Weather and Climate Extreme Events in a Changing Climate. *In* V Masson-Delmotte, P Zhai, A Pirani, SL Connors, C Péan, S Berger, N Caud, Y Chen, L Goldfarb, MI Gomis et al., eds, Climate Change 2021: The Physical Science Basis. Contribution of Working Group I to the Sixth Assessment Report of the Intergovernmental Panel on Climate Change. Cambridge University Press, Cambridge, UK and New York, NY, USA, pp. 1513–1766

Sperry J, Saliendra N (1994) Intra-and inter-plant variation in xylem cavitation in Betula occidentalis. Plant Cell Environ **17**: 1233–1241

Telewski FW, Swanson RT, Strain BR, Burns JM (1999) Wood properties and ring width responses to long-term atmospheric CO2 enrichment in field-grown loblolly pine (*Pinus taeda* L.). Plant Cell Environ **22**: 213–219

Tor-ngern P, Oren R, Ward EJ, Palmroth S, McCarthy HR, Domec JC (2015) Increases in atmospheric CO2 have little influence on transpiration of a temperate forest canopy. New Phytologist **205**: 518–525

Trueba S, Théroux-Rancourt G, Earles JM, Buckley TN, Love D, Johnson DM, Brodersen C (2022) The three-dimensional construction of leaves is coordinated with water use efficiency in conifers. New Phytologist **233**: 851–861

Woodward FI, Kelly CK (1995) The influence of CO2 concentration on stomatal density. New Phytologist **131**: 311–327

Xu Z, Jiang Y, Jia B, Zhou G (2016) Elevated-CO2 response of stomata and its dependence on environmental factors. Front Plant Sci **7**: 657

Xu Z, Shimizu H, Ito S, Yagasaki Y, Zou C, Zhou G, Zheng Y (2014) Effects of elevated CO2, warming and precipitation change on plant growth, photosynthesis and peroxidation in dominant species from North China grassland. Planta **239**: 421–435

Xu Z, Zhou G (2008) Responses of leaf stomatal density to water status and its relationship with photosynthesis in a grass. J Exp Bot **59**: 3317–3325

Zhou Y, Jiang X, Schaub M, Wang X, Han J, Han SJ, Li MH (2013) Ten-year exposure to elevated CO2 increases stomatal number of *Pinus koraiensis* and *P. sylvestriformis* needles. Eur J For Res **132**: 899–908

Zwieniecki MA, Brodribb TJ, Holbrook NM (2007) Hydraulic design of leaves: insights from rehydration kinetics. Plant Cell Environ **30**: 910–921